Int J Adv Manuf Technol (2015) 77:1889–1905
DOI 10.1007/s00170-014-6575-z

ORIGINAL ARTICLE

A novel acc-jerk-limited NURBS interpolation enhanced with an optimized S-shaped quintic feedrate scheduling scheme

Javad Jahanpour · Mohammad Reza Alizadeh

Received: 15 July 2014 / Accepted: 3 November 2014 / Published online: 22 November 2014

Abstract This paper presents a new adaptive acc-jerk-limited nonuniform rational B-spline (NURBS) interpolation method based on an optimized S-shaped C^2 quintic feedrate planning scheme. At first, the modified quintic feedrate profile for each sharp corner during the acceleration/deceleration (acc/dec) stage is constructed. To this end, two feedrate slope correction coefficients (FSCC) are introduced for zero end point acceleration and jerk conception in acc/dec stage of each sharp corner. Also, a new algorithm is recommended to compute the acc/dec stage traverse time with respect to the deceleration starting time in this paper. Then, the modified quintic feedrate scheduling scheme equipped with the FSCC is improved for the tool path containing several sharp corners. The FSCC and the deceleration starting times corresponding to all sharp corners are evaluated using an optimization method such that the total machining time to be minimized. In this paper, the pattern search algorithm equipped with the nonlinear constraint function including the acceleration and jerk limitations Matlab code is used for obtaining the optimized parameters to accomplish the acc-jerk-limited feedrate scheduling scheme along the tool path. The proposed interpolation method is performed for several case studies and compared with the previously published methods to evaluate the effectiveness of the designed adaptive acc-jerk-limited feedrate scheduling scheme. The simulation results demonstrate that the proposed interpolation algorithm is capable for providing a smooth feedrate transition for all stages of motion along the tool path and yields satisfactory performances such as total machining time and the interpolation steps.

Keywords Adaptive NURBS interpolation · Confined chord error · Acc-jerk limited · Modified S-shaped C^2 quintic feedrate · Pattern search algorithm

J. Jahanpour (✉) · M. R. Alizadeh
Department of Mechanical Engineering, Mashhad Branch, Islamic Azad University, Mashhad, Iran
e-mail: jahanpourfr@mshdiau.ac.ir

1 Introduction

Developments of parametric interpolators and feedrate scheduling techniques along a tool path are among the most important issues in CAD/CAM systems. Since nonuniform rational B-spline (NURBS) curves including minimum parameters have a special feature in designing complicated open and closed shapes, their interpolation methods have been developed in CAD/CAM applications rather than the other standard parametric curves such as B-spline and Bezier curves.

Most of interpolation algorithms for parametric curves rely on numerical integration to compute the arc length [1–12]. In particular, use of the first- and second-order approximations of Taylor series expansion are among the most representative methods in NURBS curve interpolation techniques [5–12]. But, due to their accumulation and truncation errors, it is not possible to obtain the exact arc length information using these approaches, which makes interpolation inherently a rough approximation (even at fixed feedrates) [13]. The inaccurate arc length calculation results in undesired fluctuations in feedrate.

To cope with this problem, various NURBS interpolation methods have been presented instead of Taylor's expansion method [14–20]. For instance, Tsai and Cheng [14] proposed a predictor–corrector interpolator (PCI) to control feedrate fluctuations through setting tolerance of feedrate error for either given constant or variable feedrate commands. Zhang and Song [15] advised an iterative feedrate optimization algorithm for real-time NURBS interpolation. In their work, the parametric curve is firstly approximated with the Adams–Bashforth method (ABM) and then a feedback scheme is used to maintain the feedrate fluctuations in a specified tolerance limit.

The chord error limit can be imposed on feedrate profile generation in NURBS interpolation algorithms [21–32]. For instance, Yeh and Hsu [21] suggested an adaptive NURBS interpolation algorithm, in which the feedrate was adaptively changed along the path to keep the chord error within a specified tolerance range. Zhiming et al. [22] suggested a

variable feedrate strategy based on geometric properties of tool path. Baek et al. [23] proposed a simple and fast NURBS interpolation algorithm and compared to the Taylor series interpolators. In their work, the constant chord lengths were obtained by recursive characteristics of NURBS curve. This method aims to achieve constant chord length for the circular interpolation to reduce the feedrate fluctuations.

Although the destined precision of the chord error can be satisfied by the aforementioned algorithms, sudden changes in curve's curvature would cause the acceleration/deceleration (acc/dec) and jerk to be beyond the limits. Several methods have considered acc/dec as well as chord error in their interpolation procedure [25–32]. For instance, Yong and Narayanswami [25] investigated off-line NURBS interpolation method to simultaneously keep the both chord error within a specified tolerance and the acc/dec of corner machining. Du et al. [26] presented an adaptive NURBS interpolator with real-time look-ahead function used for corner machining to meet chord error and acc/dec constraints. Sun et al. [27] recommended a NURBS interpolator method with simultaneous constraints of chord error and acc/dec for curvilinear path machining. Feng et al. [28] proposed a real-time adaptive NURBS interpolator considering axis acceleration limit to confine both the chord error and the axis acceleration.

Adaptive NURBS interpolation methods have been recently improved by the feedrate scheduling algorithms considering confined chord error and machining dynamic characteristics, i.e., acc/dec and jerk [33–47]. The main difference of the referred methods is applying different feedrate scheduling schemes during re-interpolation stage around sharp corners, crucial points with large curvature, or sensitive areas along the tool path. Tsai et al. [35] proposed a look-ahead NURBS interpolation approach including corner detection module, a jerk-limited module, and a dynamics module to take into account chord errors, feedrate fluctuations, jerks, and servo-errors simultaneously. In their work, bell-shape acc/dec planning has been adopted in the integrated look-ahead dynamics-based (ILD) interpolation algorithm to generate the feedrate profile of each divided small segments around a sharp corner. However, their method has high computational complexity [36]. In addition, their results are presented only for a quite simple geometrical path, consisting of a few splines. Nevertheless, that iterative technique achieves better accuracy while requiring less machining time compared to the adaptive-feedrate method of Tikhon et al. [9] and the curvature-feedrate interpolation proposed by Yeh and Hsu [8]. Liu et al. [37] utilized an adaptive-feedrate NURBS interpolation scheme, which meets the requirements of constant feedrate, chord accuracy, and machining dynamic constraints. In their method, throughout the re-interpolation stage, the velocity profile at the sharp corner to satisfy the specified chord error, acc/dec, and jerk limits was accommodated by a B-spline fitting method and idea of fast Fourier transform (FFT) filtering. That method gains good performance in experiments; however, complex computation is its big flaw [38]. Xu et al. [39] proposed an adaptive NURBS interpolator with real-time look-ahead function to meet the demand of machining accuracy requirement along with limited acc/dec and jerk values. In [39], the velocity profile around a corner in the acc/dec stage is generated according to the trapezoidal or triangular acc/dec profile. But, the total time of acceleration or deceleration was not considered and the recalculation of acceleration rate or jerk was based on the requirement of interpolation curve length only [40]. Du et al. [41] developed an adaptive NURBS curve interpolator with real-time and flexible acc/dec control scheme by considering preset jerk range. In that work, the feedrate sensitive was consisted of three increasing and three decreasing stages connected by a turning point with minimum feedrate. Nevertheless, the method presented in [41] used special trace back to any feedrate sensitive area, which results in a large number of total interpolation steps. Wang et al. [42] introduced the adaptive acc/dec and jerk-limited module to smooth the velocity sharp corner. In their method, the S-shaped velocity profile around the sharp corner was smoothened by digital convolution method to ensure the acceleration and jerk within a specified tolerance. However, the digital convolution approach is unable to generate various velocity profiles which are useful for CNC machine tools [43]. In addition to the above discussed feedrate scheduling approaches, the velocity profiles for the sensitive areas used in [44] and [45] have been planned based on cubic polynomial and cubic spline methods, respectively. Also, in [46], the sine-curve velocity profile was employed for each NURBS block around a sharp corner according to the block length and the given limits of acceleration and jerk. Furthermore, a combination of acc/dec control before interpolation (ADBI) and acc/dec control after interpolation (ADAI) methods along with a digital convolution technique has been performed for scheduling the feedrate in the multi-block NURBS interpolation in [47].

Based on the different theoretical/computational aspects and various constraints used in the aforementioned NURBS interpolation techniques, the most previous relevant works are summarized in Table 1.

In this paper, a novel adaptive NURBS curve interpolation with the confined chord error, acceleration, and jerk modules is proposed. At first, using exponential functions, a new strategy to construct the modified S-shaped quintic feedrate

Table 1 The summarized previous works on the NURBS interpolation techniques

Authors/ Reference	Used theoretical/computational algorithms	Considering constraint(s)
Tsai and Cheng [14]	The predictor–corrector interpolator (PCI) for either given constant or variable feedrate commands	Confined feedrate fluctuation
Zhang and Song [15]	The Adams–Bashforth method (ABM) along with a feedback scheme	Confined feedrate fluctuation
Yeh and Hsu [21]	Adaptive feedrate method along with the first-order Taylor's expansion	Confined chord error
Baek et al. [23]	Recursive method to achieve constant chord length for the circular interpolation	Constant chord length and confined feedrate fluctuation
Yong and Narayanswami [25]	Off-line NURBS interpolation along with the first-order Taylor's expansion	Chord error and acc/dec limited
Du et al. [26]	Adaptive NURBS interpolator with real-time look-ahead function and the second-order Taylor's expansion	Chord error and acc/dec limited
Sun et al. [27]	Feedrate scheduling method along with the second-order Taylor's expansion	Chord error and acc/dec limited
Feng et al. [28]	Real-time adaptive NURBS interpolator along with the second-order Taylor's expansion	Chord error and acc/dec limited
Tsai et al. [35]	Integrated look-ahead dynamics (ILD) interpolator using bell-shape acc/dec planning	Chord error, acc/dec, and jerk limited
Liu et al. [37]	Look-ahead feedrate scheduling method around a sharp corner using B-spline fitting and FFT filtering	Chord error, acc/dec, and jerk limited
Xu et al. [39]	Adaptive feedrate scheduling method around a sharp corner using trapezoidal or triangular acc/dec profile	Chord error, acc/dec, and jerk limited
Du et al. [41]	Adaptive NURBS curve interpolator with real-time acc/dec control along with the second-order Taylor's expansion	Chord error, acc/dec, and jerk limited
Wang et al. [42]	Feedrate scheduling scheme around a sharp corner using digital convolution method	Chord error, acc/dec, and jerk limited

profile around a sharp corner on the NURBS curve is presented rather than the trapezoidal- or triangular acc/dec feedrate profile used in [39]. To this end, the feedrate slope correction coefficients (FSCC) are introduced for each sharp corner during the acc/dec stage. Also, in contrast to the method presented in [39], in which the total time of acceleration or deceleration was not considered; in this paper, the a new algorithm is recommended to compute the acc/dec stage traverse time with respect to the deceleration starting time. Then, to accomplish the acc-jerk limited S-shaped feedrate scheduling scheme along the path containing several sharp corners, the slope correction coefficients along with the starting times for acc/dec stages corresponding to all sharp corners are evaluated using the pattern search algorithm to achieve the minimum total machining time.

Henceforth, the paper is organized as follows. In Sect. 2, the principle of NURBS curves and their interpolation based on the ABM are briefly reviewed. In Sect. 3, adaptive feederate with chord error limit module is presented. In Sect. 4, the acc-jerk-limited S-shaped feedrate scheduling scheme is advised for the NURBS curve as a tool path containing several sharp corners. To evaluate the performance of the proposed acc-jerk-limited NURBS interpolation method, the simulation results are discussed and compared with previous research works in Sect. 5. Finally, Sect. 6 concludes the paper.

2 Principle of NURBS curves interpolation

2.1 Review on NURBS curves

The NURBS curve of degree p, defined by given $n+1$ control points $P_0, P_1, \ldots, P_n$ with corresponding weights $w_0, w_1, \ldots, w_n$ and the knot vector $U=\{U_0, U_1, \ldots, U_m\}$ is

$$C(u) = \frac{\sum_{k=0}^{n} N_{k,p}(u) w_k P_k}{\sum_{i=0}^{n} N_{i,p}(u) w_i} = \sum_{k=0}^{n} R_{k,p}(u) P_k \quad (1)$$

where u is the curve parameter. Also, $R_{k,p}(u)$ and $N_{k,p}(u)$ are the rational B-spline and basis functions of degree p, respectively, which are described as follows [48]:

$$R_{k,p}(u)=\frac{N_{k,p}(u)w_k}{\sum_{j=0}^{n}N_{j,p}(u)w_j} \tag{2}$$

$$\begin{aligned}N_{k,0}(u)&=\begin{cases}1 & \text{if } U_k\le u<U_{k+1}\\ 0 & \text{otherwise}\end{cases}\\ N_{k,p}(u)&=\frac{u-U_k}{U_{k+p}-U_k}N_{k,p-1}(u)\\ &+\frac{U_{k+p+1}-u}{U_{k+p+1}-U_{k+1}}N_{k+1,p-1}(u)\end{aligned} \tag{3}$$

Differentiating Eq. 1 versus u will yield [49]

$$C'(u)=\frac{dC(u)}{du}=\sum_{k=0}^{n}R'_{k,p}(u)P_k=\frac{\sum_{k=0}^{n}N'_{k,p}(u)w_kP_k}{\sum_{i=0}^{n}N_{i,p}(u)w_i}-\frac{\sum_{k=0}^{n}N'_{k,p}(u)w_k\sum_{k=0}^{n}N_{k,p}(u)w_kP_k}{\left(\sum_{i=0}^{n}N_{i,p}(u)w_i\right)^2} \tag{4}$$

and

$$\begin{aligned}c''(u)&=\frac{d^2C(u)}{du^2}=\sum_{k=0}^{n}R''_{k,p}(u)P_k=\\ &\frac{\sum_{k=0}^{n}N_{k,p}(u)w_k\sum_{k=0}^{n}N''_{k,p}(u)w_kP_k-\sum_{k=0}^{n}N''_{k,p}(u)w_k\sum_{k=0}^{n}N_{k,p}(u)w_kP_k}{\left(\sum_{i=0}^{n}N_{i,p}(u)w_i\right)^2}\\ &-\frac{2\sum_{k=0}^{n}N'_{k,p}(u)w_k\left(\sum_{k=0}^{n}N_{k,p}(u)w_k\sum_{k=0}^{n}N'_{k,p}(u)w_kP_k\right)}{\left(\sum_{i=0}^{n}N_{i,p}(u)w_i\right)^3}\\ &+\frac{2\sum_{k=0}^{n}N'_{k,p}(u)w_k\left(\sum_{k=0}^{n}N_{k,p}(u)w_kP_k\sum_{k=0}^{n}N'_{k,p}(u)w_k\right)}{\left(\sum_{i=0}^{n}N_{i,p}(u)w_i\right)^3}\end{aligned} \tag{5}$$

2.2 NURBS curves interpolation based on the ABM

Based on the feedrate along a tool path, the interpolated points on the tool path are found using the interpolation procedure. For this purpose, at first, the feedrate along the NURBS curve as the tool path is expressed as follows:

$$V(t)=\frac{ds}{dt}=\frac{ds}{du}\frac{du}{dt} \tag{6}$$

where s is the arc length. Thus, we have

$$\frac{du}{dt}=\frac{V(t)}{\sqrt{\left(\frac{dC_x(u)}{du}\right)^2+\left(\frac{dC_y(u)}{du}\right)^2+\left(\frac{dC_z(u)}{du}\right)^2}} \tag{7}$$

where $C_x(u)$, $C_y(u)$, and $C_z(u)$ are the x, y, and z components of a point on the NURBS curve corresponding to the parameter u.

The closed form solution of Eq. 7 for the NURBS parameter u does not exist in general. In this paper, the NURBS interpolator is executed as follows using the ABM around the instant of $t_k=kT_s$, rather than the first- or second-order Taylor's expansion method.

$$u_{k+1}=u_k+\frac{T_s}{24}\left(55\frac{du}{dt}\Big|_{u=u_k}-59\frac{du}{dt}\Big|_{u=u_{k-1}}+37\frac{du}{dt}\Big|_{u=u_{k-2}}-9\frac{du}{dt}\Big|_{u=u_{k-3}}\right),\ k=3,4,\ldots \tag{8}$$

where T_s is the sampling period.

According to Eq. 8, the values of u_0,u_1,u_2 and u_3 are required to compute u_{k+1}. The amount of $u_0=U_0$ is often selected as zero, and the other parameters are determined by the fourth-order Runge–Kutta method by the following equation [50]:

$$u_{k+1}=u_k+\frac{T_s}{6}(f_{k1}+2f_{k2}+2f_{k3}+f_{k4}),k=0,1,2 \tag{9}$$

In which

$$\begin{aligned}f_{k1}&=f(t_k,u_k)\\ f_{k2}&=f\left(t_k+\frac{T_s}{2},u_k+\frac{T_sf_{k1}}{2}\right)\\ f_{k3}&=f\left(t_k+\frac{T_s}{2},u_k+\frac{T_sf_{k2}}{2}\right)\\ f_{k4}&=f(t_k+T_s,u_k+T_sf_{k3})\end{aligned} \tag{10}$$

After computing the curve parameter values $u_0,u_1,u_2,\ldots$ from Eqs. 8–10, the NURBS curve segments between the contiguous interpolated points corresponding to these computed curve parameter values are obtained by Eq. 1.

3 Adaptive feedrate with chord error limit module

As shown in Fig. 1a, the maximum distance between a curve segment related to two consequently interpolated points and its corresponding chord is defined as the chord error.

The interpolated points of a NURBS curve, obtained from the interpolation method presented in Sect. 2, may result in a large chord error. Due to the fact that the chord error is considered as a major error source for interpolation [4, 28], thus, in order to achieve high-machining accuracy, the chord error must be controlled under the prescribed tolerance during interpolation. The feedrate has a significant influence on the chord error. On the other hand, the chord length is closely related to the radius of curvature as well as feedrate. Thus, the relation among chord error, feedrate, and radius of curvature should be specified in the interpolation algorithms [21].

According to Fig. 1b, the chord error can be derived by the following equation [21].

$$\delta_k = \rho_k - \sqrt{\rho_k{}^2 - \left(\frac{L_k}{2}\right)^2} \tag{11}$$

where ρ_k is the radius of curvature corresponding to u_k, and L_k represents the distance between the interpolated points $R(u_k)$ and $R(u_{k+1})$ on the arc. These parameters are calculated as follows.

$$\rho_k = \frac{\left(C'(u_k)\right)^3}{\left|C'(u_k) \times C''(u_k)\right|} \tag{12}$$

$$L_k = c(u_{k+1}) - c(u_k) = T_s \times V(u_k) \tag{13}$$

Substituting Eq. 13 into Eq. 11 yields:

$$V(u_k) = \frac{2}{T_s}\sqrt{\rho_k{}^2 - (\rho_k - \delta_k)^2} \tag{14}$$

According to Eq. 14, $V(u_k)$ is evaluated as the acceptable feedrate by setting $ER_k = \delta_k$ as the tolerance value of the chord error. Nevertheless, in the vicinity of the sharp corner with high curvature, the chord error generated by the interpolation process may exceed the prescribed tolerance. Therefore, the feedrate should be adjusted adaptively based on the curvature radius regarding the specified tolerance value of the chord error. That is

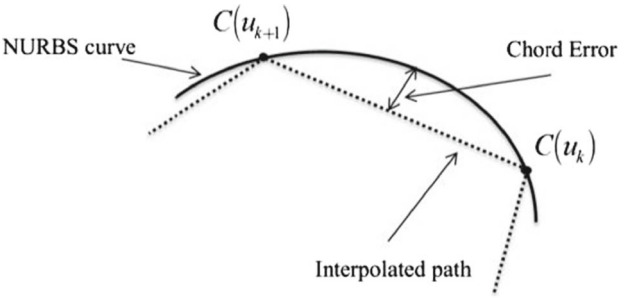

a The chord error

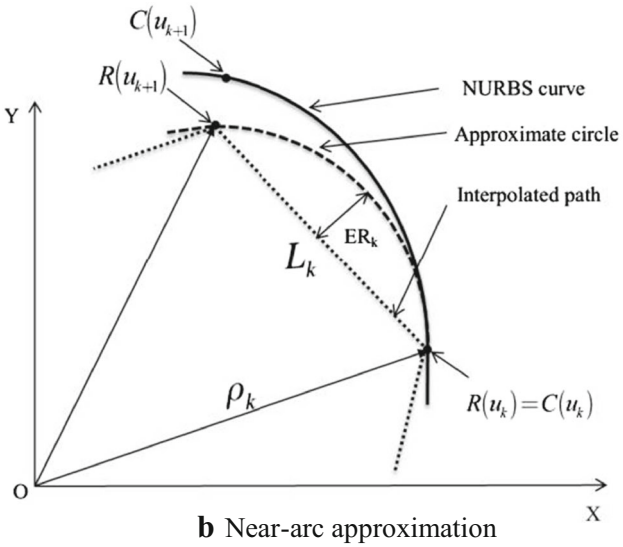

b Near-arc approximation

Fig. 1 The chord error calculation

$$V(u_k) = \begin{cases} F, \ if \ \frac{2}{T_s}\cdot\sqrt{\rho_k{}^2 - (\rho_k - ER_k)^2} > F \\ \frac{2}{T_s}\cdot\sqrt{\rho_k{}^2 - (\rho_k - ER_k)^2}, \ \text{otherwise} \end{cases} \tag{15}$$

where F is the namely feedrate along the tool path.

The sensitive feedrate area corresponding to the large curvature points of the path is divided to two typical stages as deceleration and acceleration, which are connected by a turning point with the minimum feedrate of $V_{\min}$ obtained from the adaptive feedrate with chord error limit module. The feedrate profile in the vicinity of a sharp corner can be represented as follows:

$$\{V(u_k) = F, V(u_{k+1}), \ldots, V(u_{k+m}) = V_{\min}, \ldots, V(u_{k+m+n}), V(u_{k+m+n+1}) = F\}$$

where u_{k+m} refers to the parameter value of the velocity sharp corner point with minimum feedrate of $V_{\min}$.

4 The proposed feedrate scheduling scheme enhanced with the confined acceleration and jerk modules

During the interpolation process, the feedrate is adjusted based on the adaptive feedrate with chord error limit module. However, the adaptive feederate based on the chord error limit for the crucial points with large curvatures may lead to the amount of acc/dec and jerk along the path exceeds their allowable tolerance range. This work causes some problems such as heavy shock to machine tool and subsequently deteriorates surface quality and machining accuracy as well [41]. In addition to considering the adaptive feederate based on the chord error limit, in the following, a new confined acc-jerk feedrate scheduling scheme is proposed to improve the NURBS curve interpolation procedure. In the proposed algorithm, the namely feedrate is maintained at most of the time and adaptively reduced in large curvature areas to meet the demand of the confined acceleration and jerk as well as the chord error.

The advised feedrate scheduling scheme for each stage of acc/dec around a sharp corner consists of the following modules:

- The modified S-shaped quintic feedrate construction module
- The acc/dec stage traverse time calculation module
- The optimized acc-jerk-limited S-shaped quintic feedrate scheduling scheme module

In the following, at first, a brief review on the time-dependent acc/dec feedrate profiles is presented. Then, a new strategy to construct the modified S-shaped quintic feedrate profile around a sharp corner for each stage of acc/dec is introduced. Finally, the optimized acc-jerk-limited S-shaped quintic feedrate scheduling scheme is elaborated.

4.1 Time-dependent acc/dec feedrate profiles

Consider a time-dependent feedrate function $V(t)$ defined on the acc/dec stage around a sharp corner. Note that $t\in[0,T]$, where T is the traverse time. A specific simple form of variable federate V is a polynomial of t, and it is very useful to achieve smooth feed acceleration (deceleration). Using the normalized time variable $\tau=t/T$ and expressing $V(t)$ in the Bernstein basis form on the unit interval $\tau\in[0,1]$, we have [51]

$$V(\tau)=\sum_{k=0}^{n} V_k b_k^n(\tau) \tag{16}$$

where $b_k^n(\tau)=\binom{n}{k}(1-\tau)^{n-k}\tau^k$ and V_k are the Bernstein basis functions and coefficients, respectively.

Given a polynomial $V(t)$ of odd degree n in Eq. 16, one can define a feedrate profile that matches $V=V_i$ for $t\le 0$ and $V=V_f$ for $t\ge T$ with $C^{(n-1)/2}$ continuity. In order to obtain smooth motion transition between different phases along the path and also ensure continuity of both the feed acceleration (deceleration) and feed jerk, the S-curve C^2 quintic profiles are preferred rather than the C^0 linear and C^1 cubic ones [51, 52].

For the C^2 quintic time-dependent feedrate profile, the Bernstein coefficients V_k in Eq. 16 are determined by applying the conditions of speed, acceleration, and jerk at the beginning of acc/dec stage, i.e., $V_i, \dot{V}_i$ and $\ddot{V}_i$, and the end of acc/dec stage, i.e., $V_f, \dot{V}_f$ and $\ddot{V}_f$ [51]. Those are

$$\begin{aligned}
V_0 &= V_i\\
V_1 &= V_i+\frac{1}{5}T\dot{V}_i\\
V_2 &= V_i+\frac{2}{5}T\dot{V}_i+\frac{1}{20}T^2\ddot{V}_i\\
V_3 &= V_f-\frac{2}{5}T\dot{V}_f+\frac{1}{20}T^2\ddot{V}_f\\
V_4 &= V_f-\frac{1}{5}T\dot{V}_f\\
V_5 &= V_f
\end{aligned} \tag{17}$$

Figure 2 shows the C^2 quintic variable feedrate deceleration profile defined by Eqs. 16 and 17 when $V_0=V|_{\tau=0}=V_i$, $V_5=V|_{\tau=1}=V_f$, and $\dot{V}_i=\dot{V}_f=\ddot{V}_i=\ddot{V}_f=0$.

4.2 The modified quintic feedrate profile around a sharp corner using exponential functions

Although the Bernstein coefficients in Eq. 17 yields a unique smooth feedrate profile in acc/dec stage via Eq. 16, which meets the requirements of initial and final values of feedrate, acceleration, and jerk, there is no control on the ace/dec and jerk values during the traverse time. These coefficients can be modified to achieve an S-shaped quintic feedrate profile around a sharp corner, which affect the acceleration and jerk during the specified traverse time.

In this paper, a new strategy to construct the S-shaped quintic feedrate profile around a sharp corner for each stage of acceleration or deceleration is introduced. This strategy is based on zero end point acceleration and jerk conception in each acc/dec stage. In fact, the sharp corner along the path is passed through such that the acceleration and jerk values at the start and end points of acc/dec stage during the traverse time to be zero, i.e., $\ddot{V}_i|_{\tau=0}=0$, $\ddot{V}_f|_{\tau=1}=0$, $\dot{V}_i|_{\tau=0}=0$, $\dot{V}_f|_{\tau=1}=0$.

To satisfy the above acceleration and jerk conditions by the S-shaped quintic feedrate profile, the following time-dependent end-acc/dec and end-jerk conditions are proposed:

$$\begin{aligned}
V_i &= 1-e^{(n_a\tau)}\\
V_f &= 1-e^{n_a(1-\tau)}\\
\dot{V}_i &= 1-e^{(n_j\tau)}\\
\dot{V}_f &= 1-e^{n_j(1-\tau)}
\end{aligned} \tag{18}$$

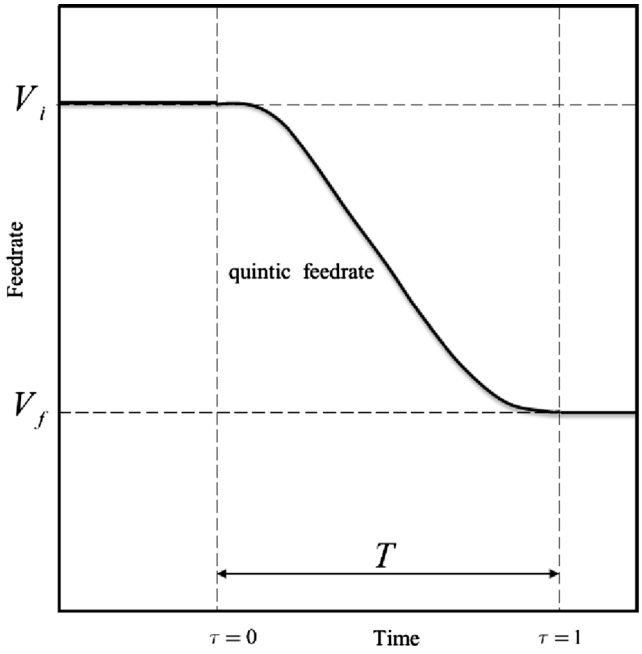

Fig. 2 Feed deceleration from V_i to V_f using the C^2 quintic feedrate defined by Eqs. 16 and 17

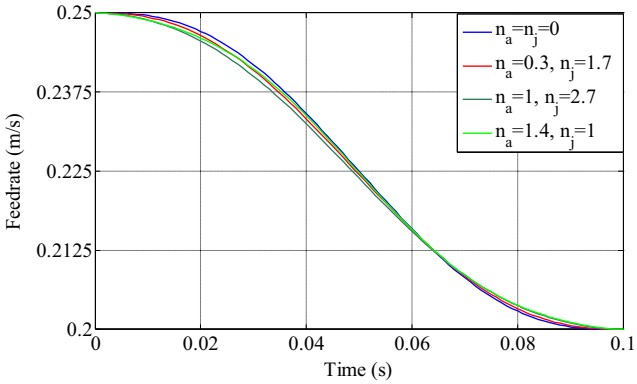

Fig. 3 The effect of FSCC on the deceleration feedrate profile during a specified traverse time

where n_a and n_j are the FSCC for a sharp corner during the acc/dec stage.

Using the end-acc/dec and end-jerk conditions via Eq. 18 in Eq. 17 and substituting the newly Bernstein coefficients into Eq. 16 yields the modified quintic feedrate profile as $V(\tau, n_a, n_j)$ around a sharp corner during the traverse time period.

In order to investigate the effect of the FSCC, i.e., the set of n_a and n_j, on the C^2 quintic feedrate profile, Fig. 3 is illustrated. Figure 3 shows the modified quintic feedrate profiles within the traverse time of T=0.1 s from V_i=0.25 m/s to V_f=0.2 m/s for several different values of n_a and n_j. As can be seen in Fig. 3, the feedrate at the end points of a sharp corner in the deceleration stage are kept as $V_i=V_i|_{\tau=0}$=0.25 m/s and $V_f=V_f|_{\tau=1}$= 0.2 m/s, while the feedrate slope during the specified traverse time is varied. Subsequently, the acceleration and the jerk during the traverse time T=0.1 s are changed. Therefore, the FSCC defined for a sharp corner has the significant effect on the slope of the feedrate profile within a certain traverse time. In the other words, the acceleration and the jerk values during the traverse time depends on the FSCC utilized in the proposed modified quintic feedrate profile around the sharp corner.

4.3 Acc/dec stage traverse time calculation for a sharp corner

The acc/dec stage traverse time, i.e., T, has the important role to construct the acc-jerk-limited S-shaped quintic feedrate profile around a sharp corner. Because the acceleration and deceleration stage traverse time calculation has the same procedure, in the following, the deceleration stage traverse time calculation process is explained.

According to Fig. 4a, point B has namely velocity of F and denotes to the start point of the adaptive feedrate. This point is evaluated using the adaptive feedrate with chord error limit module Eq. 15. Besides, point C refers to the end point of the adaptive feedrate with chord error limit module, i.e., the minimum feedrate of $V_{\min}$ related to the sharp corner. The adaptive feedrate time t_{clm} is determined having points B and C. Figure 4a also shows the specifications of the modified quintic feedrate profile including a specified set of n_a and n_j around a sharp corner in the deceleration stage. In fact, the proposed modified quintic feedrate profile with the confined chord error, acceleration and jerk modules is constructed between the points A and D as shown in Fig. 4a. For a given starting time t_A, the trace back time t_1 and consequently point A can be easily determined by indexing of the interpolated points on the constant namely feedrate of F with respect to the point B.

As shown in Fig. 4b, A′, B′, C′, and D′ are points on the path via the NURBS curve corresponds to the points A, B, C, and D on the feedrate profile, respectively. As it is observed, for a given starting time t_A, all points A,B, C, and D on the adaptive feedrate profile equipped with the chord error limit module are obtained. Thus, the distance from A′ to C′, i.e., $\overline{A'C'}$, is calculated using the adaptive feedrate profile with chord error limit module. According to Fig. 4b, the trace back distance from A′ to D′ employing the proposed modified quintic feedrate profile must be equal to the distance from A′ to C′ using the adaptive feedrate profile with chord error limit module. Therefore, the area under their corresponding points on the aforementioned feedrate profiles should be equal. That is

$$S_{ADEG} = S_{ABCFG} = \overline{A'C'} \tag{19}$$

It is noted that $S_{ADEG} = \int_0^{\tau=t/T} V(\tau, n_a, n_j)d\tau$, in which $V(\tau,n_a,n_j)$ is the modified quintic feedrate profile via Eq. 16 along with the time-dependent end-acc/dec and end-jerk conditions of Eq. 18.

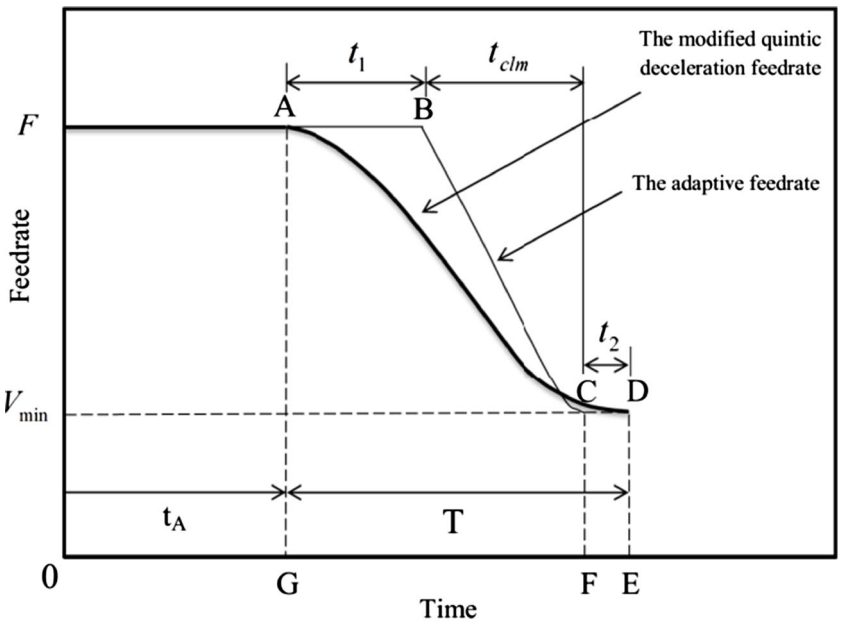

a Specifications of the modified quintic feedrate profile

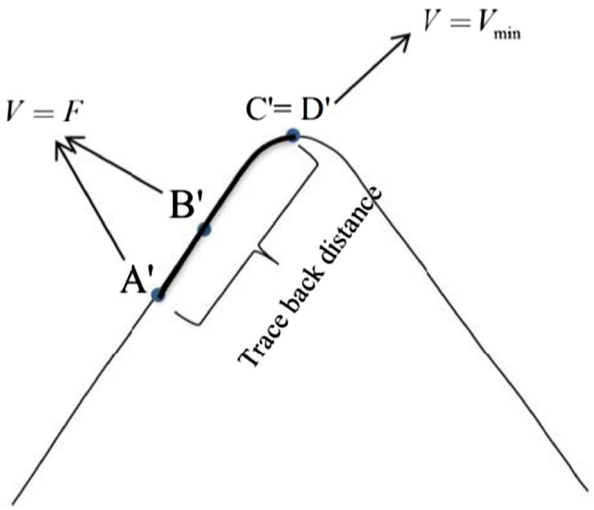

b Typical sharp corner with trace back distance

Fig. 4 The modified quintic feedrate profile around a sharp corner in the deceleration stage

After obtaining the adaptive feedrate profile with chord error limit module, for a given starting time t_A, n_a and n_j corresponding to a sharp corner, the deceleration stage traverse time T is computed from Eq. 19. Also, the trace forward time t_2 is evaluated as $t_2 = T - t_1 - t_{clm}$.

4.4 The optimized acc-jerk-limited S-shaped feedrate scheduling scheme

In general, as shown in Fig. 5, the tool path contains several sharp corners, which should be passed through with the modified quintic acc/dec feedrate profiles. According to Fig. 5, three independent parameters as n_{ai}, n_{ji} and t_{Ai} are employed to construct the modified quintic feedrate profile around the sharp corner #i in each acc/dec stage. Therefore, to accomplish the S-shaped quintic feedrate scheduling scheme along the path, the FSCC and the starting acc/dec times corresponding to all sharp corners, i.e., n_{ai}, n_{ji} and t_{Ai} for $i = 1, \ldots n$, should be specified. As a result, $3n$ parameters must be used for constructing all modified quintic acc/dec feedrate profiles on the path containing n sharp corners. These parameters can be determined using an optimization algorithm such that the total machining time be minimized while the acc/dec and jerk limit constraints are satisfied.

The total machining time as the objective function (O.F.) throughout use of the S-shaped quintic feedrate scheduling

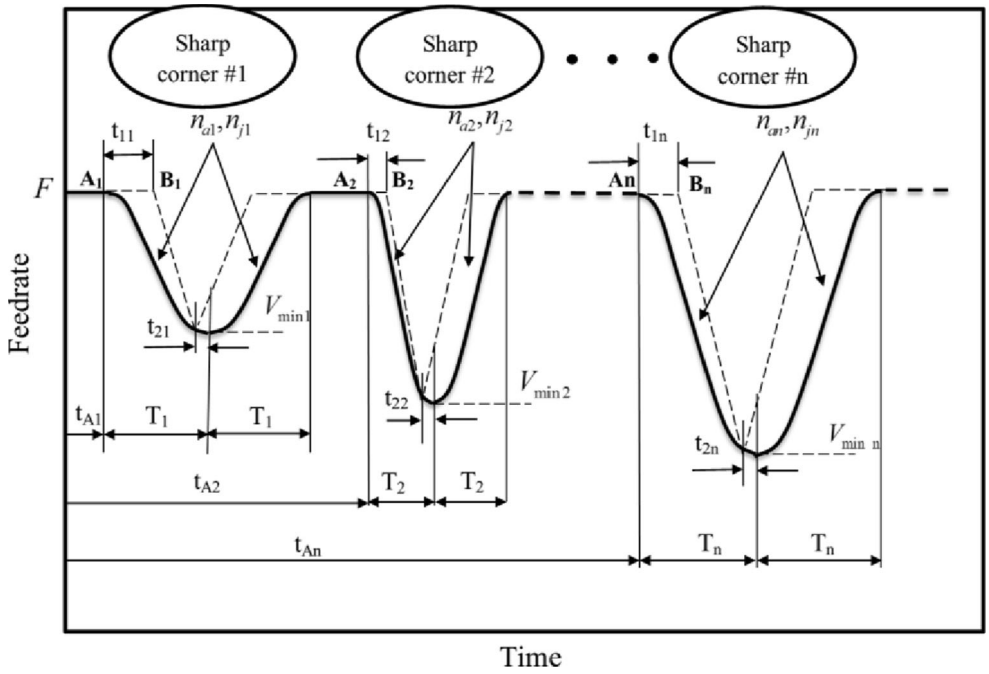

Fig. 5 The S-shaped quintic feedrate scheduling scheme along the path containing several sharp corners

scheme along the path does not have the implicit function, and it is computed numerically. Besides, the derivative of the objective function is not available and also it is impossible to obtain explicit estimation of any derivatives of the objective function as well as the objective function. Therefore, the direct search methods can be used for solving the aforementioned optimization problems in which does not require any information about the gradient of the objective function.

There are three direct search methods called the generalized pattern search (GPS), the generating set search (GSS), and the mesh adaptive search (MADS). All are pattern search algorithms that compute a sequence of points at each step, which is called a mesh, that approach an optimal point. The mesh is formed by adding the current point to a scalar multiple of a set of vectors called a pattern. With GPS, the collections of vectors that form the pattern are fixed-direction vectors. With GSS, the pattern is identical to the GPS pattern, except when there are linear constraints and the current point is near a constraint boundary. Also, with MADS, the collection of vectors that form the pattern are randomly selected by the algorithm. Further details on the pattern search algorithm can be found in [53, 54].

The GPS method as the pattern search algorithm is employed in this paper to achieve the optimized total machining time. The Matlab code: pattern search(@O.F.,X0,LB,UB, NonlCon) minimizes the O.F. using the starting point X0 subjected to a set of lower and upper bounds on the design variables (LB and UB) under the nonlinear constraints defined in NonlCon function. The solution X is found in the range LB≤X≤UB.

The following nonlinear constraints for the acc/dec and jerk values must be used in our optimization algorithm. Thus,

$$\{acc/dec\&jerk\}_{\text{actual}}\text{-}\{acc/dec\&jerk\}_{\text{allowable}}\leq 0 \qquad (20)$$

In this work, NonlCon is the nonlinear constraint function presented by Eq. 20. A Matlab function NonlCon is written to keep the maximum acc/dec and jerk within the specified allowable physical limits throughout the Matlab's pattern search algorithm in our optimization problem. The selected options for the pattern search algorithm are chosen according to [55, 56]. The outputs of the pattern search algorithm are the optimum variables and the minimized total machining time. In fact, the proposed interpolation method profits from the optimization algorithm equipped with the nonlinear constraint function, in which the requirements of the machining dynamic are satisfied via Eq. 20. Thus, the machining dynamic constraints have been taken into account in the advised acc-jerk-limited interpolation method.

According to the flowchart depicted in Fig. 6, the optimization variables are n_{ai},n_{ji} and t_{Ai}. The pattern search algorithm starts with an initial point for n_{ai},n_{ji} and t_{Ai}. In stage 1, based on initial amounts of n_{ai},n_{ji} and t_{Ai}, the deceleration stage traverse time for the first sharp corner, i.e., T_1, is computed using Eq. 19. In stage 2, the modified quintic feedrate profile around the first sharp corner in the deceleration stage with the traverse time T_1 is constructed. In this stage, the modified quintic feedrate profile around the first sharp corner in the acceleration stage is also constructed. This work is done

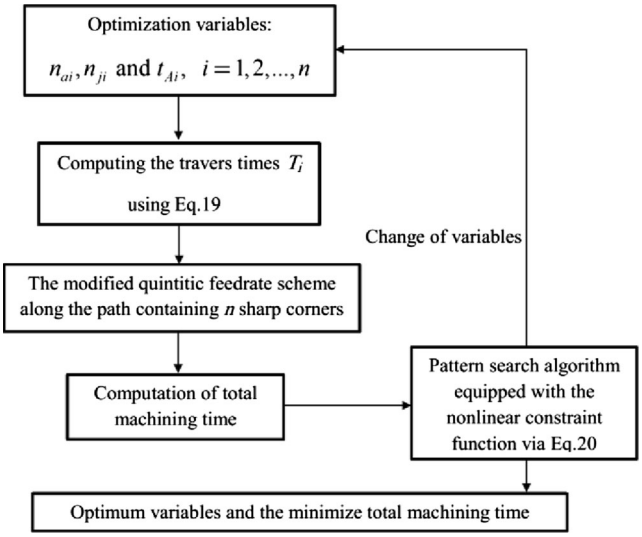

Fig. 6 The pattern search algorithm implemented for minimization of the total machining time

for all sharp corners along the NURBS curve as the tool path to complete the modified quintic feedrate scheme. In the next stage, the total machining time, which is the sum of the acc/dec stage times around all sharp corners and the time related to the all constant feedrate stages of motion, are computed for a set of n_{ai},n_{ji} and t_{Ai}. At each successful iteration, the pattern search algorithm changes the variable via the nonlinear constraint function Eq. 20. Finally, the minimized total machining time and the optimum variables are computed by the pattern search algorithm equipped with the nonlinear constraint function Eq. 20.

In this paper, the distance between adjacent sharp corners along the tool path is considered long enough such that they do not overlap. It should be noted that there are different types of overlapping corners called "ripple effect" of adjacent corners/sensitive points [57]. For instance, the feedrate profile in the acceleration phase around a corner may intersect with the feedrate profile in the deceleration phase around the adjacent corner, or in another type, the whole feedrate profile around a corner may be replaced with the adjacent corner's feedrate profile, and so on. Thus, based on the different relationship of the adjacent sharp corners, the proposed acc-jerk-limited interpolation method should be improved to update the start point of deceleration, the end point of acceleration phase, and the feedrate profiles around two consecutive corners.

Due to the fact that the machining dynamic constraints in this work have been included in the optimization algorithm equipped with the nonlinear constraint function, the proposed acc-jerk-limited interpolation method has much lower complexity than the other methods in which the dynamic constraints are directly considered in the interpolation algorithms. Nevertheless, cause of utilizing an optimization algorithm which is inherently time consuming, for the case of very long tool path in practical applications, calculation load may be large. For that case; an off-line carrying out of the algorithm leads to state the feedrate profiles around sharp corners on the tool path and subsequently, for real-time interpolation, the parametric curve information can be augmented with the detected feedrate profiles.

5 Performance analysis and simulation results

5.1 Case studies

Two NURBS curves as case studies are used to evaluate the performance of the proposed feedrate scheduling scheme with the confined chord error, acceleration and jerk modules. One is the "diamond"-shaped curve and the other is "infinity"-shaped curve. The degree, knot vector, control points, and the weights for constructing the diamond curve are chosen according to [39], while these parameters to generate the infinity-shaped curve are selected according to [41]. Those are as follows:

Diamond curve,

$$
\begin{aligned}
&p = 2\\
&U = \{0,0,0,0.25,0.25,0.5,0.5,0.75,0.75,1,1,1\}\\
&P_0 = (0.15,0.3,0), P_1 = (0.3,0.4,0), P_2 = (0.45,0.3,0),\\
&P_3 = (0.6,0.2,0), P_4 = (0.45,0.1,0), P_5 = (0.3,0,0),\\
&P_6 = (0.15,0.1,0),\ P_7 = (0,0.2,0),\ P_8 = (0.15,0.3,0)\\
&w_0 = 1, w_1 = 10, w_2 = 1, w_3 = 10, w_4 = 1,\\
&w_5 = 10, w_6 = 1, w_7 = 10, w_8 = 1
\end{aligned}
$$

Infinity curve,

$$
\begin{aligned}
&p = 2\\
&U = \{0,0,0,0.25,0.5,0.5,0.75,1,1,1\}\\
&P_0 = (0.15,0.15,0), P_1 = (0,0,0), P_2 = (0,0.3,0),\\
&P_3 = (0.15,0.15,0), P_4 = (0.3,0,0), P_5 = (0.3,0.3,0),\\
&P_6 = (0.15,0.15,0)\\
&w_0 = 1, w_1 = 100, w_2 = 100, w_3 = 1, w_4 = 100,\\
&w_5 = 100, w_6 = 1
\end{aligned}
$$

As can be seen in Fig. 7a, the diamond-shaped curve contains four large curvature corners marked as 1, 2, 3, and 4, and the directional change in corners 2 and 4 is sharper than that of 1 and 3, while the infinity has four sharp corners with the same curvatures (see Fig. 7b). The curvature of two above NURBS curves are also depicted in Fig. 7c. The starting point for the interpolating the diamond- and Infinity-shaped curves are also shown in Fig. 7a, b. The simulation conditions for interpolating the above curves are given in Table 2 based on [39, 41].

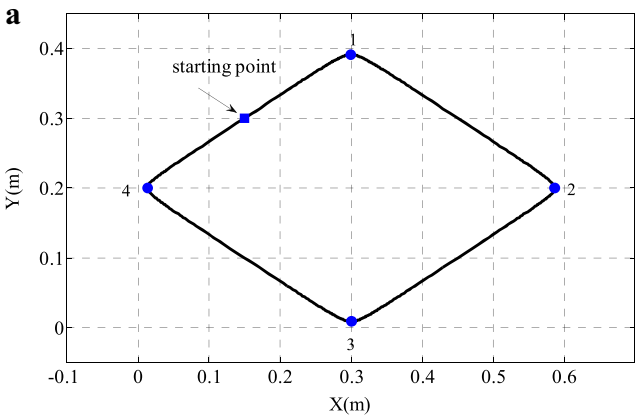

Fig. 7 The diamond- and infinity-shaped as the NURBS curves used in the simulation tasks

5.2 Interpolation results

5.2.1 Diamond interpolation

The diamond curve has the same curvature in corners 1 and 3 as well as corners 2 and 4. Therefore, the same n_a and n_j are considered for the sharp corners with same curvatures. For this case, eight independent optimization variables as t_{A1},t_{A2},t_{A3}, t_{A4}, $n_{a1}=n_{a3}$,$n_{a2}=n_{a4}$, $n_{j1}=n_{j3}$, and $n_{j2}=n_{j4}$ are computed by the pattern search algorithm. The start point, lower bounds, and upper bounds of these parameters used in the pattern search algorithm are given in Table 3. As reported in Table 3, for this case, the start point, lower bounds, and upper bounds of the parameters in the pattern search algorithm for minimizing the total machining time are as follows:

$$X_0 = [0.65;\ 2.0;\ 3.75;\ 5.2;\ 0.05;\ 0.9;\ 0.1;\ 0.4;\ 0.05;\ 0.9;\ 0.1;\ 0.4]$$
$$LB = [0.6;\ 1.8;\ 3.3;\ 4.5;\ 0.01;\ 0.01;\ 0.01;\ 0.01;\ 0.01;\ 0.01;\ 0.01;\ 0.01]$$
$$UB = [0.9;\ 2.3;\ 3.9;\ 5.4;\ 1;\ 1;\ 1;\ 1;\ 1;\ 1;\ 1;\ 1]$$

For the diamond interpolation, the parameters of the optimized acc-jerk-limited S-shaped feedrate have been computed by the pattern search algorithm as presented in Table 4. Those are as follows:

$$t_{A1} = 0.746, t_{A2} = 2.08359, t_{A3} = 3.6776,\ t_{A4} = 5.0141$$
$$n_{a1} = n_{a3} = 0.09\ ,\ n_{a2} = n_{a4} = 0.19$$
$$n_{j1} = n_{j3} = 0.69\ ,\ n_{j2} = n_{j4} = 0.59$$

The results of the pattern search algorithm for this case are shown in Fig. 8. As can be seen, the total machining time using the above initial point is equal to 6.3 s, which converges and reduces to 6.19 s after 105 iterations. The total number of function evaluations is equal to 1596.

The simulation results for the diamond interpolation using the proposed acc-jerk-limited feedrate scheduling scheme are illustrated in Fig. 9. Figure 9a shows the optimized acc-jerk-limited S-shaped feedrate along the path. The adaptive feedrate profile obtained from the chord error limit module is also depicted in Fig. 9a. It is observed that the chord error calculated by the optimized acc-jerk-limited S-shaped feedrate is less than its allowable tolerance limit, i.e., 1 μm (see Fig. 9b). The resulting feedrate and the chord error profiles from the acc-jerk-limited NURBS interpolation enhanced with the optimized S-shaped C^2 quintic feedrate planning

Table 2 The interpolation conditions for the diamond- and infinity-shaped curves

	Diamond [39]	Infinity [41]
Namely feedrate	F= 0.25 m/s	F= 0.2 m/s
Maximum acceleration	A_{max}= 1 m/s^2	A_{max}=1 m/s^2
Maximum jerk	J_{max}= 10 m/s^3	J_{max}= 10 m/s^3
Maximum chord error	δ_{max}= 1 μm	δ_{max}=1 μm
Sampling period	T_s=2 ms	T_s=2 ms

Table 3 Start point, lower bounds, and upper bounds of the parameters in the pattern search algorithm

	Diamond			Infinity		
	Lower	Start	Upper	Lower	Start	Upper
t_{A1}	0.6	0.65	0.9	0.5	0.75	0.9
t_{A2}	1.8	2.0	2.3	1.95	2.2	2.5
t_{A3}	3.3	3.75	3.9	3.9	4.1	4.6
t_{A4}	4.5	5.2	5.4	5.7	6	6.2
n_{a1}	0.01	0.05	1	0.01	0.5	1
n_{j1}	0.01	0.9	1	0.1	0.5	1
n_{a2}	0.01	0.1	1	0.01	0.5	1
n_{j2}	0.01	0.4	1	0.1	0.5	1
n_{a3}	0.01	0.05	1	0.01	0.5	1
n_{j3}	0.01	0.9	1	0.1	0.5	1
n_{a4}	0.01	0.1	1	0.01	0.5	1
n_{j4}	0.01	0.4	1	0.1	0.5	1

scheme show that the feedrate automatically reduces at large curvature areas to confine the dynamic characteristics (see inset of Fig. 9a). Also, it is found that the minimum feedrate at the first (third) corner is $V_{\min 1} = V_{\min 3} = 0.2121 \frac{m}{s}$, while this value for the second (fourth) corner is $V_{\min 2} = V_{\min 4} = 0.1155 \frac{m}{s}$. That is, the larger the curvature results in the lower the feedrate.

Figure 9c, d presents the acceleration and jerk profile along the diamond-shaped curve obtained from the proposed interpolation algorithm. Figure 9c, d describes three main phases of motion as the first acceleration phase from start to reach the namely feedrate, middle region of motion and the last deceleration phase from the namely feedrate to stop. The maximum amounts of the acceleration and jerk in the middle region of the motion have been computed as $0.9039 \frac{m}{s^2}$ and $9.986 \frac{m}{s^3}$. These maximum values of the acceleration and jerk do not exceed their maximum allowable limits of $1 \frac{m}{s^2}$ and $10 \frac{m}{s^3}$. The

Table 4 The optimized parameters of the acc-jerk-limited S-shaped feedrate computed by the pattern search algorithm

	Diamond	Infinity
t_{A1}	0.746	0.8137
t_{A2}	2.08359	2.3416
t_{A3}	3.6776	4.4974
t_{A4}	5.0141	6.0306
n_{a1}	0.09	0.1155
n_{j1}	0.69	0.4058
n_{a2}	0.19	0.1155
n_{j2}	0.59	0.4058
n_{a3}	0.09	0.1155
n_{j3}	0.69	0.4058
n_{a4}	0.19	0.1155
n_{j4}	0.59	0.4058

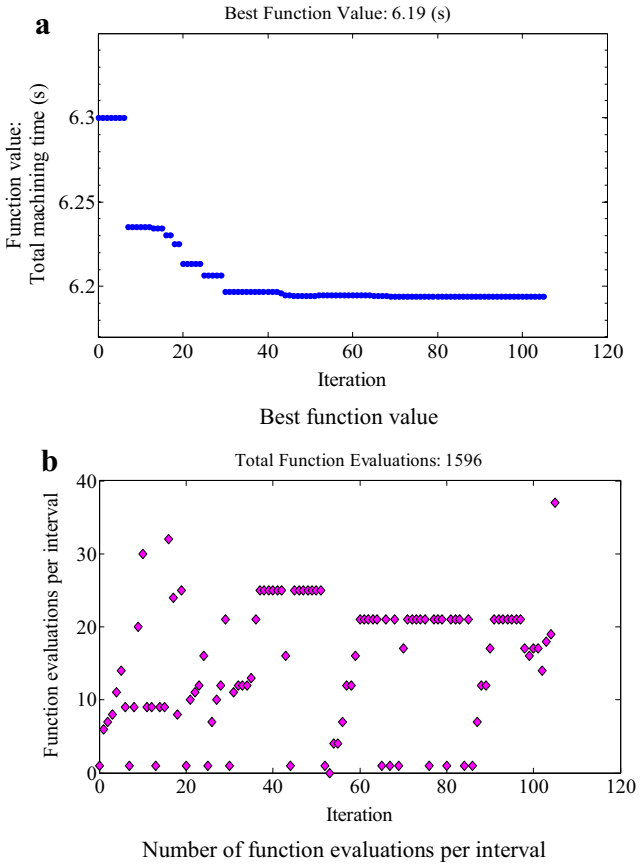

Fig. 8 The pattern search algorithm results for the diamond-shaped interpolation

marked points in Fig. 9c (Fig. 9d) refer to the zero acceleration (zero jerk) points along the path. These points are due to the proposed zero end point acceleration and jerk strategy and are related to the start and end of the acceleration and the deceleration stages around each sharp corner.

The interpolation results for the diamond obtained from the proposed interpolation algorithm including the total machining time and the interpolation steps are presented in Table 5. These results are also compared with the acc-jerk-limited adaptive interpolation method given in [39]. According to Table 5, for the diamond-shaped interpolation, the total machining time using the proposed acc-jerk-limited interpolation algorithm is 6.19 s, which is comparable to the total machining time obtained from the acc-jerk-limited adaptive interpolation method proposed by [39]. In addition, the interpolation steps using the proposed acc-jerk-limited interpolation algorithm is 3098, that is closed to the corresponding result presented in [39].

5.2.2 Infinity interpolation

The infinity curve has the same curvature in all corners. Therefore, the same n_a and n_j are considered for all sharp corners. For this case, six independent optimization variables

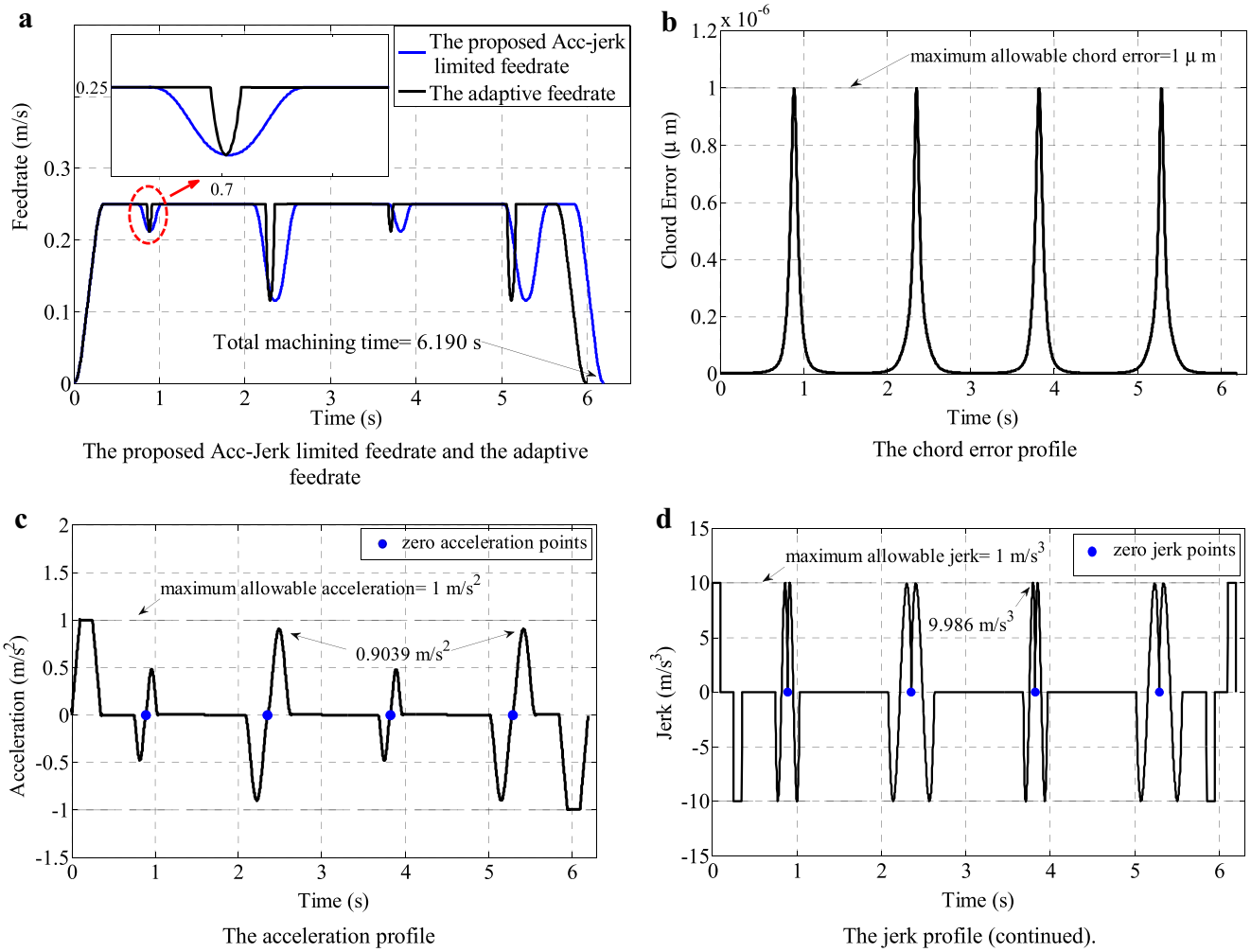

Fig. 9 The interpolation results for the diamond-shaped curve obtained from the proposed acc-jerk-limited method

as t_{A1},t_{A2},t_{A3},t_{A4}, n_{a1}=n_{a2}=n_{a3}=n_{a4}, and n_{j1}=n_{j2}=n_{j3}=n_{j4} are computed by the pattern search algorithm. The start point, lower bounds, and upper bounds of these parameters used in the pattern search algorithm are also given in Table 3.

For the infinity interpolation, according to Table 4, the parameters of the optimized acc-jerk-limited S-shaped feedrate have been computed by the pattern search algorithm as follows:

$$t_{A1} = 0.8137, t_{A2} = 2.3416, t_{A3} = 4.4974, t_{A4} = 6.0306$$
$$n_{a1} = \quad n_{a2} = \quad n_{a3} = \quad n_{a4} = \quad 0.1155$$
$$n_{j1} = \quad n_{j2} = \quad n_{j3} = \quad n_{j4} = \quad 0.4058$$

It is found that the total machining time using the initial point given in Table 3 converges to 7.3682 s after 132 iterations and 1038 function evaluations.

The simulation results for the infinity interpolation using the proposed acc-jerk-limited feedrate scheduling scheme are illustrated in Fig. 10. Figure 10a shows the optimized acc-jerk-limited S-shaped feedrate along the path. The adaptive feedrate profile is also depicted in this figure. It is observed that the chord error obtained by the optimized acc-jerk-limited S-shaped feedrate is less than its allowable tolerance limit of 1 μm (see Fig. 10b). The minimum feedrate at all sharp corners as shown in Fig. 10a is $V_{\min 1} = V_{\min 2} = V_{\min 3} = V_{\min 4} = 0.0752 \frac{m}{s}$.

Figure 10c, d presents the acceleration and jerk profile along the infinity-shaped curve obtained from the proposed interpolation algorithm. As can be seen in Fig. 10c, d, the maximum amounts of the acceleration and jerk are obtained as $-0.8649 \frac{m}{s^2}$ and $-9.916 \frac{m}{s^3}$, respectively, which are less than their corresponding maximum allowable limits of $1 \frac{m}{s^2}$ and $10 \frac{m}{s^3}$. For the case of infinity-shaped curve, the total machining time and the interpolation steps have also been presented in Table 5. These results are also compared with the acc-jerk-limited adaptive interpolation method proposed by [41]. According to Table 5, for the infinity-shaped curve, the obtained total machining time using the proposed acc-jerk-limited interpolation algorithm is 7.368 s, which is better compared to the total machining time obtained from the acc-jerk-limited adaptive interpolation method given in [41]. In addition, the

Table 5 Total machining time and interpolation steps using different adaptive interpolator algorithms

		Acc-jerk-limited adaptive method presented in [39]	Acc-jerk-limited adaptive method presented in [41]	The proposed adaptive acc-jerk-limited method
Diamond	Machining time	6.194 s	–	6.190 s
	Interpolation steps	3097	–	3098
Infinity	Machining time	–	7.414 s	7.368 s
	Interpolation steps	–	3707	2980

interpolation steps using the proposed acc-jerk-limited interpolation algorithm with the optimized S-shaped C^2 quintic feedrate planning scheme is 2980, that is lower than its amount using the three increasing/three decreasing stages feedrate sensitive profile presented in [41]. The lower number of interpolation steps has significant practical advantages. In particular; for some practical applications such as real-time contour following tasks with a high performance controller, the lower interpolation steps decreases the complexity of implementation algorithm as well as the contour following time.

In the following, further advantages of the developed algorithm over the previously existing methods are presented.

In contrast with the method presented in [39, 41], in which the deceleration starting point and re-plan the feedrate around each sharp corner were evaluated based on several complex preconditions for employed trapezoidal or triangular profile; in this paper, the starting point and the feedrate profile around corners are optimized by the optimization algorithm. On the other hand, as it is observed in Figs. 9d and 10d, the jerk profiles obtained from the proposed acc-jerk-limited interpolation method are extremely smoother than the jerk profiles

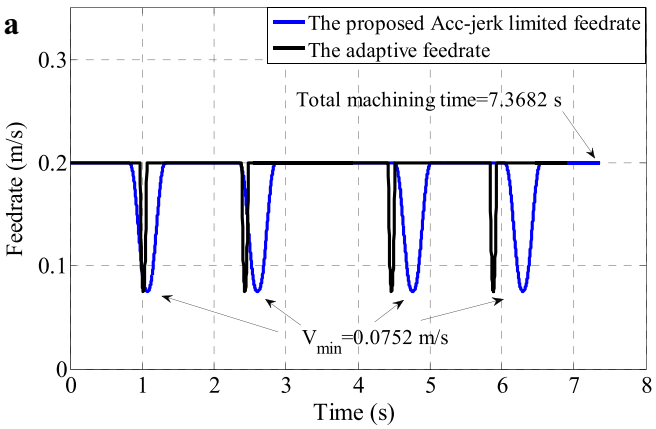

The proposed Acc-Jerk limited feedrate and the adaptive feedrate

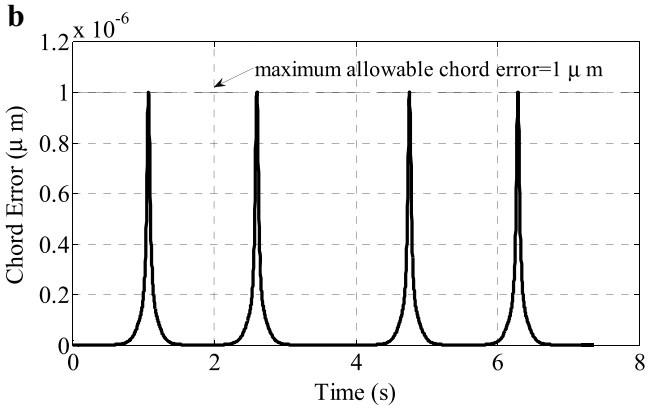

The chord error profile

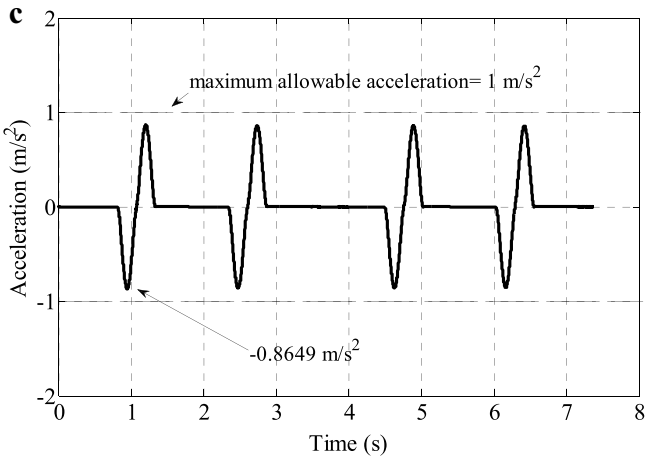

The acceleration profile (continued).

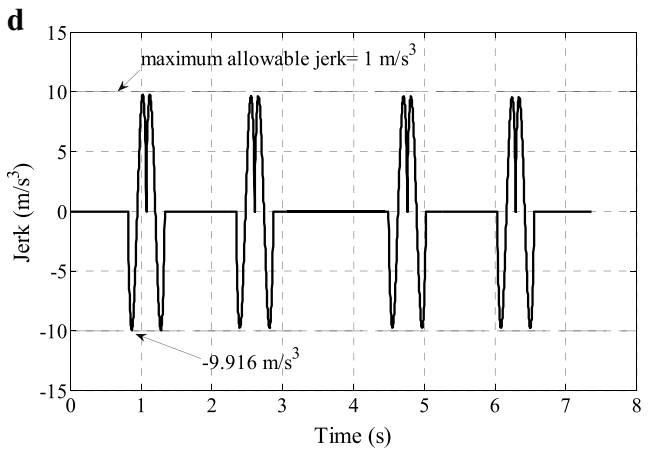

The jerk profile (continued).

Fig. 10 The interpolation results for the infinity-shaped curve obtained from the proposed acc-jerk-limited method

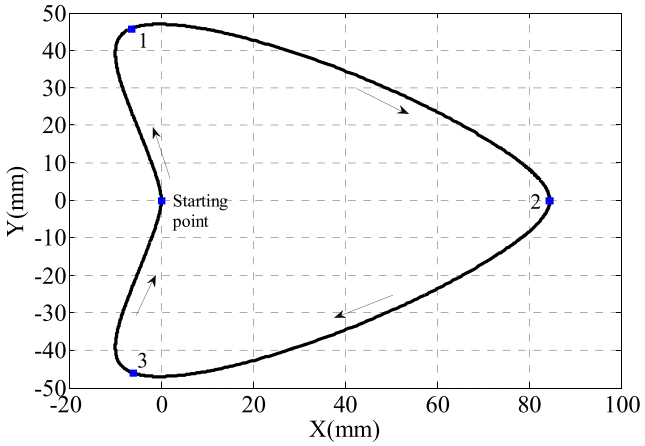

Fig. 11 The heart-shaped as the NURBS curve

found by the methods presented in [39, 41]. In addition, as can be seen in Figs. 9d and 10d, the jerk profiles are close to the specified maximum values just for a number of points along the tool path, while the trapezoidal and triangular feedrate profiles used in [39, 41] cause the maximum jerk value is obtained in most of the time along the tool path. Therefore, in contrast with the method given in [39, 41], due to a low number of points in achieving the maximum allowable jerk value in the proposed algorithm, the advised method substantially reduces the mechanical shock to the machine tool and improves the machining quality as well.

In order to compare the advised interpolation method with the C^2 PH B-spline curve interpolator adopted in [52], the "heart"-shaped curve is illustrated. The conditions for the heart curve interpolation are selected according to [52] as $F = 100$ mm/s and $T_s = 1$ ms. Also, the parameters to generate the heart-shaped curve are as follows:

$$
\begin{aligned}
&p = 3\\
&U = \left\{0,0,0,0,1\Big/6,2\Big/6,3\Big/6,4\Big/6,5\Big/6,1,1,1,1\right\}\\
&P_0 = (0,0,0), P_1 = (10,0,0), P_2 = (-20,50,0),\\
&P_3 = (40,50,0), P_4 = (90,0,0), P_5 = (40,-50,0),\\
&P_6 = (-20,-50,0), P_7 = (0,-10,0), P_8 = (0,0,0)\\
&w_0 = 1, w_1 = 1, w_2 = 1.7, w_3 = 1, w_4 = 4,\\
&w_5 = 1, w_6 = 1.7, w_7 = 1, w_8 = 1
\end{aligned}
$$

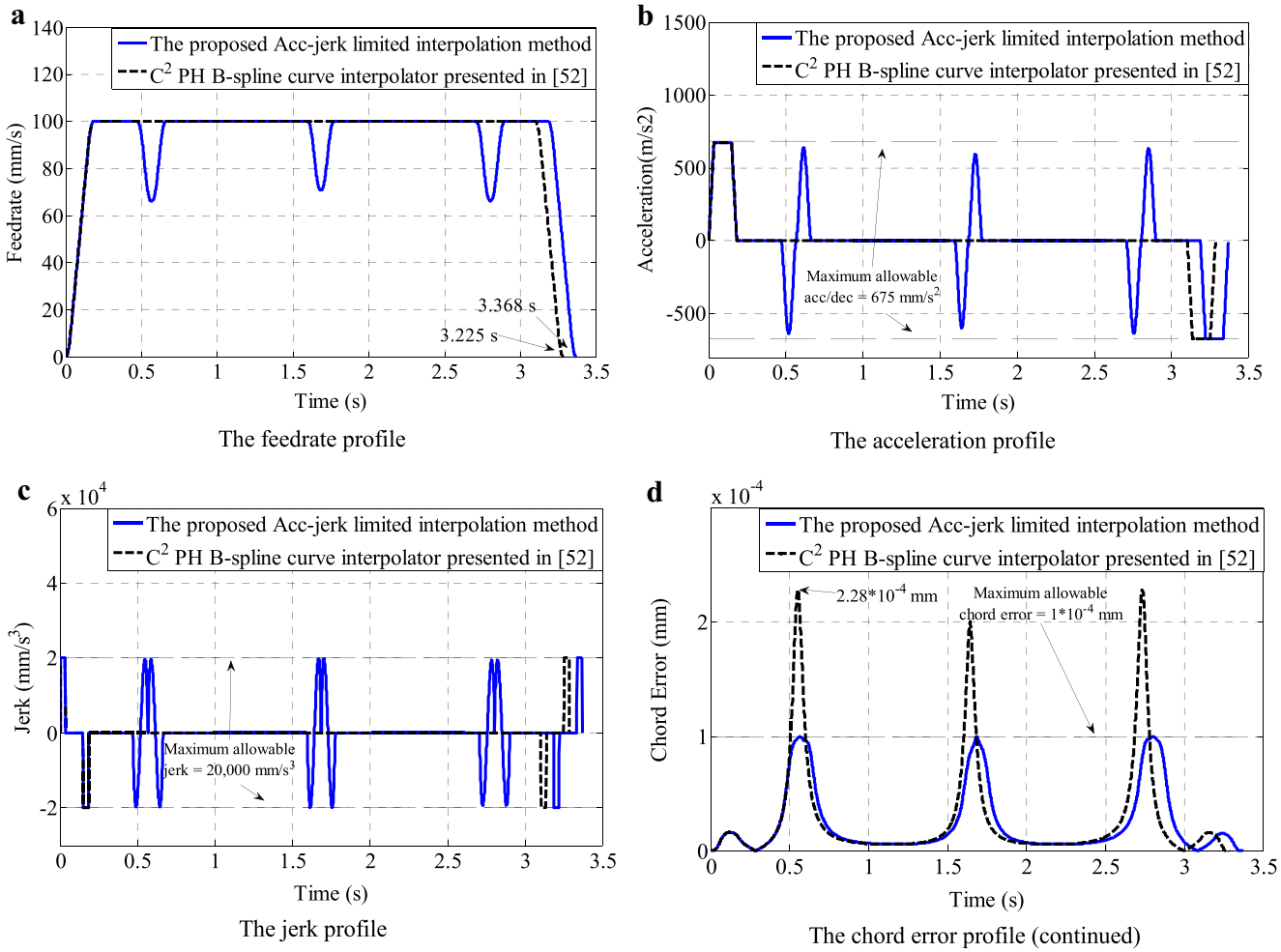

Fig. 12 Comparison the interpolation results for the heart-shaped curve obtained from the proposed acc-jerk-limited method with the algorithm presented in [52]

As can be seen in Fig. 11, the heart-shaped curve contains three large curvature corners marked as 1, 2, and 3. The curvature profile for the heart curve was given in [52]. Using the above parameters and the C^2 PH B-spline curve interpolator, the feedrate, acc/dec, jerk, and chord error profiles along the heart-shaped curve are obtained. These profiles are shown as the dashed curves in Fig. 12. Based on the C^2 PH B-spline curve interpolation algorithm, the above large curvature corners on the tool path passed through with the constant namely feedrate of $F = 100$ mm/s (see dashed profile in Fig. 12a). Thus, the interpolation procedure in [52] yields a large amount of chord error in these corners. As it shown in Fig. 12d, the maximum chord error using the C^2 PH B-spline curve interpolator is 2.28×10^{-4} mm. Moreover, the motion planning scheme in [52] was provided such that the acceleration and jerk were zero during the constant feedrate phase of motion, and the maximum acceleration and jerk occurred in the acc/dec phase of motion. In fact, the method presented in [52] yields the confined acc/dec and jerk values along the tool path; however, there is no control on chord error during the interpolation. For the case of heart-shaped curve, the maximum amounts of acceleration and jerk are 675 mm/s^2 and 20,000 mm/s^3, respectively (see dashed profiles in Fig. 12b, c).

The heart-shaped curve is also interpolated by the proposed acc-jerk-limited interpolation method with the same constraints of A_{max}=675 mm/s^2, J_{max}=20,000 mm/s^3, and additional constraint for the chord error as $\delta_{max} = 1 \times 10^{-4}$ mm. As it can be seen in Fig. 12, the proposed acc-jerk-limited interpolation method supplies the confined chord error, acceleration, and jerk, simultaneously. Furthermore, as it is observed in Fig. 12b, c, the newly advised interpolation algorithm profits from the allowable tolerance limits of the acceleration and jerk in the constant feedrate phase of motion compared to the motion planning scheme given in [52]. As shown in Fig. 12a, although the total machining time using the acc-jerk-limited interpolation method is increased by a small amount of 4.4 % with respect to the interpolation method presented in [52], the requirements of chord error and machining dynamic constraints have been met.

6 Conclusions

This paper has introduced a new acc-jerk-limited NURBS interpolation method enhanced with the optimized feedrate scheduling scheme. At first, employing the FSCC, the S-shaped C^2 quintic feedrate profile was constructed under zero end point acceleration and jerk conditions for each sharp corner during the acc/dec stage. For this aim, a new algorithm was also advised for computing the acc/dec stage traverse. Then, the proposed feedrate scheduling scheme was improved for the tool path containing several sharp corners. In this paper, the feedrate slope correction coefficients and the deceleration starting times corresponding to all sharp corners have been evaluated using the pattern search algorithm equipped with the nonlinear constraints of acceleration and jerk to minimize the total machining time. Therefore, the proposed acc-jerk-limited NURBS interpolation method effectively reduces the machining shocks. The proposed acc-jerk-limited NURBS interpolation method was performed for the diamond- and infinity-shaped curves as case studies. The interpolation results demonstrated that the feedrate automatically reduces at large curvature areas to confine the dynamic characteristics as well as chord error within their specified limits. Besides, the simulation results for the diamond- and infinity-shaped curves confirm that the optimized S-shaped C^2 quintic feedrate planning scheme is significantly capable for providing a smooth feedrate transition for all stages of motion along the tool path. Moreover, the proposed acc-jerk-limited feedrate scheduling scheme not only feasible for adaptive NURBS curve interpolation but also yields satisfactory performance such as the total machining time and the interpolation steps compared to the previously published methods. Future work will mainly focus on the acc-jerk-limited NURBS interpolation method considering the ripple effect in the tool path.

References

1. Erkorkmaz K, Altintas Y (2005) Quintic spline interpolation with minimal feed fluctuation. ASME J Manuf Sci Eng 127(2):339–349
2. Wang FC, Wright PK (1998) Open architecture controllers for machine tools, part 2: a real time quintic spline interpolator. ASME J Manuf Sci Eng 120(2):425–432
3. Sekar M, Narayanan VN, Yang SH (2008) Design of jerk bounded feedrate with ripple effect for adaptive nurbs interpolator. Int J Adv Manuf Technol 37(5–6):545–552
4. Park J, Nam S, Yang M (2005) Development of a real-time trajectory generator for NURBS interpolation based on the two-stage interpolation method. Int J Adv Manuf Technol 26(4):359–365
5. Koren Y, Lo CC, Shpitalni M (1993) CNC interpolators: algorithms and analysis. ASME PED J Manuf Sci Eng 64:83–92
6. Shipitalni M, Koren Y, Lo CC (1994) Real- time curve interpolators. Comput Aided Des 26(11):832–838
7. Yang DCH, Kong T (1994) Parametric interpolator versus linear interpolator for precision CNC machining. Comput Aided Des 26(3):225–234
8. Yeh SS, Hsu PL (1999) The speed-controlled interpolator formachining parametric curves. Comput Aided Des 31:349–357
9. Tikhon M, Ko TJ, Lee SH, Kim HS (2004) NURBS interpolator for constant material removal rate in open NC machine tools. Int J Mach Tools Manuf 44:237–245
10. Cheng CW, Tsai MC (2004) Real-time variable feedrate NURBS curve interpolator for CNC machining. Int J Adv Manuf Technol 23(11–12):865–873
11. Su KH, Cheng MY (2008) Contouring accuracy improvement using cross-coupled control and position error compensator. Int J Mach Tools Manuf 48:1444–1453

12. Cheng MY, Su KH, Wang SF (2009) Contour error reduction for free-form contour following tasks of biaxial motion control systems. Robot Comput Integr Manuf 25(2):323–333
13. Farouki RT, Tsai YF (2001) Exact Taylor series coefficients for variable-feedrate CNC curve interpolators. Comput Aided Des 33: 155–165
14. Tsai MC, Cheng CW (2003) A real-time predictor corrector interpolator for CNC machining. Trans J Manuf Sci Eng 125:449–460
15. Zhang XT, Song Z (2012) An iterative federate optimization method for real-time NURBS interpolator. Int J Adv Manuf Technol 62: 1273–1280
16. Lei WT, Sung MP, Lin LY, Huang JJ (2007) Fast real-time NURBS path interpolation for CNC machine tools. Int J Mach Tools Manuf 47(10):1530–1541
17. Liu J, Chen B, Liu M, Xu D, Li Y (2012) An optimization of NURBS interpolation algorithm. 10th IEEE International Conference 316–319
18. Jeong SY, Choi YJ, Park PG (2006) Parametric interpolation using sampled data. Comput Aided Des 38:39–47
19. Wu JC, Zhou HC, Tang XQ, Chen JH (2012) A NURBS interpolation algorithm with continuous federate. Int J Adv Manuf Technol 59: 623–632
20. Yau HT, Lin MT, Tsai MS (2006) Real-time NURBS interpolation using FPGA for high speed motion control. Comput Aided Des 38: 1123–1133
21. Yeh S, Hsu P (2002) Adaptive-feedrate interpolation for parametric curves with a confined chord error. Comput Aided Des 34:229–237
22. Zhiming X, Jincheng C, Zhengjin F (2002) Performance evaluation of real-time interpolation algorithm for NURBS curves. Int J Adv Manuf Technol 20:270–276
23. Baek DK, Yang SH, Ko TJ (2012) Precision NURBS interpolator based on recursive characteristics of NURBS. Int Adv Manuf Technol 65:403–410
24. Liang H, Wang YZ, Li X (2006) Implementation of an adaptive feed speed 3D NURBS interpolation algorithm. Front Mech Eng China 4: 403–408
25. Yong T, Narayanaswami R (2003) A parametric interpolator with confined chord errors, acceleration and deceleration for NC machining. Comput Aided Des 35:1249–1259
26. Du DS, Liu YD, Yan C, Li C (2007) An accurate adaptive parametric curve interpolator for NURBS curve interpolation. Int J Mach Tools Manuf 32:999–1008
27. Sun YW, Jia ZY, Ren F, Guo DM (2008) Adaptive feedrate scheduling for NC machining along curvilinear paths with improved kinematic and geometric properties. Int J Adv Manuf Technol 36:60–68
28. Feng J, Li Y, Wang Y, Chen M (2010) Design of a real-time adaptive NURBS interpolator with axis acceleration limit. Int J Adv Manuf Technol 48:227–241
29. Luo FY, Zhou YF, Yin J (2007) A universal velocity profile generation approach for high-speed machining of small line segments with look-ahead. Int J Adv Manuf Technol 35:505–518
30. Zhang K, Yuan CM, Gao XS (2013) Efficient algorithm for time-optimal feedrate planning and smoothing with confined chord error and acceleration. Int J Adv Manuf Technol 66(9):1685–1697
31. Sun Y, Zhou J, Guo D (2013) Variable feedrate interpolation of NURBS Toolpath with geometric and kinematical constraints for five-axis CNC machining. J Syst Sci Complex 26:757–776
32. Zhou J, Sun Y, Guo D (2014) Adaptive feedrate interpolation with multiconstraints for five-axis parametric toolpath. Int J Adv Manuf Technol 71:1873–1882
33. Nam SH, Yang MY (2004) A study on a generalized parametric interpolator with real time jerk-limited acceleration. Comput Aided Des 36(1):27–36
34. Lai JY, Lin KY, Tseng SJ, Ueng WD (2008) On the development of a parametric interpolator with confined chord error, feedrate, acceleration and jerk. Int J Adv Manuf Technol 37(1–2):104–121
35. Tsai MS, Nien HW, Yau HT (2008) Development of an integrated look-ahead dynamics-based NURBS interpolator for high precision machinery. Comput Aided Des 40:554–566
36. Rutkowski L, Przybył A, Cpałka K (2012) Novel on-line speed profile generation for industrial machine tool based on flexible neuro-fuzzy approximation. EEE Trans Ind Electron 59(2):1238–1247
37. Liu X, Ahmad F, Yamazaki K, Mori M (2005) Adaptive interpolation scheme for NURBS curves with the integration of machining dynamics. Int J Mach Tools Manuf 45(4–5):433–444
38. Shen HY, Fu JZ, Fan YQ (2011) A new adaptive interpolation scheme of NURBS based on axis dynamics. Int J Adv Manuf Technol 56:215–221
39. Xu RZ, Xie L, Xi LCX, Du DS (2008) Adaptive parametric interpolation scheme with limited acceleration and jerk values for NC machining. Int J Adv Manuf Technol 36:343–354
40. Ni XY, Wang DH, Li YB (2011) Real-time NURBS curve interpolator based on section. Int J Adv Manuf Technol 54(1–4):239–249
41. Du DS, Liu YD, Guo XG, Yamazaki KZ, Fujishima M (2010) An accurate adaptive NURBS curve interpolator with real-time flexible acceleration/deceleration control. Robot Comput Integr Manuf 26(4): 273–281
42. Wang X, Wang J, Rao Z (2010) An adaptive parametric interpolator for trajectory planning. Adv Eng Softw 41:180–187
43. Dong HT, Chen B, Chen YP, Xie JM, Zhou ZD (2012) An accurate NURBS curve interpolation algorithm with short spline interpolation capacity. Int J Adv Manuf Technol 63:1257–1270
44. Annoni M, Bardine A, Campanelli S, Foglia P, Prete CA (2012) A real-time configurable NURBS interpolator with bounded acceleration, jerk and chord error. Comput Aided Des 44:509–521
45. Wang YQ, Liu H, Yu S (2012) Curvature-based real-time NURBS surface interpolator with look-ahead ACC/DEC control. Math Comput Sci 6:315–326
46. Lee AC, Lin MT, Pan YR, Lin WY (2011) The feedrate scheduling of NURBS interpolator for CNC machine tools. Comput Aided Des 43(6):612–628
47. Tsai MS, Nien HW, Yau HT (2011) Development of integrated acceleration/deceleration look-ahead interpolation technique for multi-blocks NURBS curves. Int J Adv Manuf Technol 56:601–618
48. Piegl L (1991) On NURBS: a survey. IEEE Comput Graph 11(1):55–71
49. Piegl LA, Tiller W (1995) The NURBS book. Springer, New York
50. Yang WY, Cao W, Chung TS, Morris J (2005) Applied numerical methods using MATLAB. Wiley-Interscience, Hobokon
51. Tsai YF, Farouki RT, Feldman B (2001) Performance analysis of CNC interpolators for time-dependent feed rates along PH curves. Comput Aided Geom Des 18(3):245–265
52. Jahanpour J, Tsai M-C, Cheng M-Y (2010) High-speed contouring control with NURBS-based C^2 PH spline curves. Int J Adv Manuf Technol 49:663–674
53. Lewis RM, Torczon V (1999) Pattern search algorithms for bound constrained minimization. SIAM J Optim 9(4):1082–1099
54. Direct Search Toolbox, MathWorks, Inc. (2006). http://www.mathworks.com
55. Jahanpour J, Imani BM (2008) Real-time P-H curve CNC interpolators for high speed cornering. Int J Adv Manuf Technol 39(3–4):302–316
56. Jahanpour J, Ghadirifar A (2014) The improved NURBS-based C^2 PH spline curve contour following task with PDFF controller. Int J Adv Manuf Technol 70:995–1007
57. Wang H, Zhao D (2009) Research and implementation of NURBS real-time and look-ahead interpolation algorithm. Int Conf Meas Technol Mechatron Autom ICMTMA 09:273–276